3652 J. Phys. Chem. 1990, 94, 3652-3656

Kinetics of the Reaction between Oxygen Atoms and Allyl Radicals

I. R. Slagle, J. R. Bernhardt, D. Gutman,*

Department of Chemistry, Catholic University of America, Washington, D.C. 20064

M. A. Hanning-Lee, and M. J. Pilling*,†

Physical Chemistry Laboratory, Oxford University, South Parks Road, Oxford OX1 3QZ, United Kingdom
(Received: September 12, 1989; In Final Form: December 4, 1989)

The reaction between C_3H_5 and $O(^3P)$ has been studied over the temperature range 300–600 K by using two time-resolved techniques: laser flash photolysis of $C_3H_5Br/SO_2/He$ mixtures at 193 nm with detection by photoionization mass spectrometry, and laser flash photolysis of $C_6H_{10}/N_2O/N_2$ mixtures at 193 nm using absorption spectroscopy and resonance fluorescence to detect C_3H_5 and O, respectively. A temperature and pressure (2–350 Torr) independent rate constant of $(3 \pm 1) \times 10^{-10}$ cm^3 molecule^{-1} s^{-1} was obtained. Acrolein was the only product detected by photoionization mass spectrometry, suggesting that the major channel is $C_3H_5 + O \rightarrow C_3H_4O + H$.

I. Introduction

The allyl radical (C_3H_5) is an important intermediate formed during the pyrolysis and oxidation of hydrocarbons.[1-5] Because of its exceptional stability, it is often present at significant concentrations both in flames and in high-temperature pyrolysis processes.[3,4] While many reactions which produce C_3H_5 have been identified and characterized (e.g., the abstraction of the methyl hydrogen from propene by atoms and free radicals),[3,6] those that consume it during high-temperature pyrolysis and oxidation processes have not.[2] This resonance-stabilized free radical resists pyrolysis[4] as well as high-temperature oxidation by molecular oxygen,[7] the two processes that account for most of the loss of polyatomic free radicals under these conditions.[2]

It has been concluded that C_3H_5 is largely consumed by the more abundant atoms and free radicals (R) found in flames and other combustion systems. Several such reactions have been suggested as being important, e.g., reactions with HO_2, H, CH_3, CH_3O_2, OH, and O.[2,3,6] None of these reactions have been investigated to determine its mechanism and rate constant parameters. In the global reaction mechanisms that have been used to account for the observable properties of flames and other combustion processes, likely products of C_3H_5 + R reactions have been proposed and rate constants either estimated or used as adjustable parameters.

Studies of the $C_3H_5 + C_3H_5$ recombination reaction have shown that this association has a rate constant comparable to that of alkyl–radical recombination reactions.[8] Therefore, it appears that the resonance stabilization of C_3H_5 does not reduce the rates of radical–radical reactions in which it is a participant. If this is generally the case, then the C_3H_5 + R reactions mentioned above should, under appropriate conditions, be important sinks for this radical in combustion processes.

We have now investigated the kinetics of one of these reactions, C_3H_5 + O. Rate constants have been determined as a function of temperature and density over a significant range of conditions by using two independent methods. In addition, an important reaction channel has been identified.

The C_3H_5 + O reaction is expected to begin with the formation of an energy-rich alkenoxy radical, $C_3H_5O^*$. The internal energy of $C_3H_5O^*$ is large, ≈419 kJ mol^{-1}, enough for a variety of decomposition processes to occur, including simple bond cleavage and internal H atom migration (followed by decomposition into different sets of products). A special effort was made to search for a pressure dependence in the rate constant, which, if present and determined, would provide a measure of the lifetime of $C_3H_5O^*$.

II. Experimental Section

Two independent experimental approaches were used to measure the C_3H_5 + O rate constant. The two methods employ different photolysis sources of C_3H_5 and use substantially different concentrations of the two reactants. They also cover complementary pressure ranges. The first technique involves the use of a tubular reactor coupled to a photoionization mass spectrometer with which both reactants and products can be observed in time-resolved experiments. This facility was also used to search for and identify reaction products. In the second method, reactant gases are flowed slowly through a large-diameter reactor, which is essentially wall-less at the pressures and time scales used. Both reactants are detected simultaneously in time-resolved mode: O by atomic resonance fluorescence and C_3H_5 by ultraviolet absorption.

A. Studies Using Photoionization Mass Spectrometry To Monitor C_3H_5 and Reaction Products. Details of the experimental facility[9] and the procedure used to measure rate constants of O + R reactions have been published[10,11] and are therefore only briefly reviewed here. Pulsed unfocused 193-nm radiation (≈5 Hz) from a Lambda Physik EMG 201 MSC excimer laser was directed along the axis of a heatable 1.05-cm-i.d. quartz tubular reactor coated with boric acid to reduce heterogeneous loss of oxygen atoms. Gas passing through the tube at ≈4 m s^{-1} was completely replaced between laser pulses. The flowing gas contained SO_2 (the O atom source; <0.05 %), allyl bromide (the C_3H_5 source; typically 0.0005%), and the carrier gas He, which was always in great excess (>99.9%). Gas was sampled through a 0.043-cm-diameter hole located at the end of a nozzle in the wall of the reactor and formed into a beam by a conical skimmer before it entered the vacuum chamber containing the photoionization mass spectrometer. As the gas beam traversed the ion source, a portion was photoionized and mass selected. Temporal ion signal profiles were recorded from a short time before each laser pulse

---

† Present address: University of Leeds, Physical Chemistry Department, Leeds LS2 9JT, United Kingdom.

(1) Cathonnet, M.; Boettner, J. C.; James, H. *Symp. (Int.) Combust. [Proc.], 18th* **1981**, 903.

(2) Westbrook, C. K.; Dryer, F. L. *Prog. Energy Combust. Sci.* **1984**, *10*, 1.

(3) Westbrook, C. K.; Pitz, W. J. *Combust. Sci. Technol.* **1984**, *37*, 117.

(4) Edelson, D.; Allara, D. L. *Int. J. Chem. Kinet.* **1980**, *12*, 605.

(5) Smith, R. D. *J. Phys. Chem.* **1979**, *83*, 1553.

(6) Wilk, R. D.; Cernansky, N. P.; Pitz, W. J.; Westbrook, C. K. *Combust. Flame*, in press.

(7) Slagle, I. R.; Gutman, D. *Symp. (Int.) Combust. [Proc.], 21st* **1986**, 875.

(8) Tulloch, J. M.; Macpherson, M. T.; Morgan, C. A.; Pilling, M. J. *J. Phys. Chem.* **1982**, *86*, 3812.

(9) Slagle, I. R.; Gutman, D. *J. Am. Chem. Soc.* **1985**, *107*, 5342.

(10) Slagle, I. R.; Sarzynski, D.; Gutman, D. *J. Phys. Chem.* **1987**, *91*, 4375.

(11) Slagle, I. R.; Sarzynski, D.; Gutman, D.; Miller, J. A.; Melius, C. F. *J. Chem. Soc., Faraday Trans. 2* **1988**, *84*, 491.

0022-3654/90/2094-3652$02.50/0 © 1990 American Chemical Society

TABLE I: Conditions and Results of Experiments To Measure the C_3H_5 + O Rate Constant Using Photoionization Mass Spectrometry

T, K	10^{-16}[He], molecules cm^{-3}	$10^{-10}[C_3H_5]_0$, molecules cm^{-3}	$10^{-11}[O]_0$, molecules cm^{-3}	k_3, s^{-1}	k_4, s^{-1}	$10^{10}k_2$,[b] cm^3 molecule s^{-1}
296	6.06	0.5–1.6	3.6–13.0	2.1	16.1	3.4
295	12.0	0.5–1.7	2.6–15.1	3.3	13.8	3.5
360[c]	6.02	0.6–1.7	3.1–16.0	3.0, 4.2	13.3, 13.4	3.0
360	12.0	0.6–2.3	3.0–16.2	2.3	11.0	3.1
450	6.02	0.6–1.9	3.9–16.1	12.3	13.3	3.2
450	12.1	0.5–1.0	3.7–15.4	11.9	12.7	3.3
600[c]	6.03	0.6–2.8	3.8–19.7	12.2, 8.4	6.4, 5.6	2.8
600[a]	12.0	0.4–2.1	5.1–16.7	18.4, 7.0	10.8, 4.4	2.6

[a] Set of experiments displayed in Figure 1. [b] Estimated maximum probable uncertainty, ±25%. [c] Double entries for k_3 and k_4 are from sets of experiments performed over a 2-day period. These heterogeneous loss rate constants were remeasured on the second day with the new values being used in the data analysis of the later experiments.

to 25 ms following the pulse with a multichannel scaler. Data from 2000 to 14 000 repetitions of the experiment were accumulated before the data were analyzed.

1. Photolysis of Allyl Bromide. In virtually all the experiments, C_3H_5Br was the C_3H_5 source. The 193-nm photolysis of this compound proceeds by two major routes:

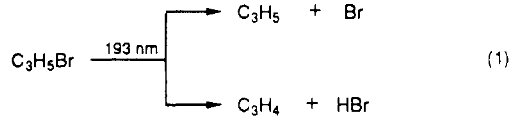

(1)

The relative importance of the two paths was not measured, but, based on product ion signal intensities, both routes appear to be of comparable significance. The initial C_3H_5 concentrations selected were so low (typically 2×10^{10} molecules cm^{-3})[12] that reactions between photolysis products (including the $C_3H_5 + C_3H_5$ reaction) had negligible rates. The presence of Br, C_3H_4, and HBr did not interfere with either the rate constant determinations or the search for reaction products.

2. Measurement of C_3H_5 + O Rate Constants. The experiments to measure the O + C_3H_5 rate constant were conducted like those in the study of the O + CH_3 reaction[11] in which it was shown that 193-nm photolysis of SO_2 was a clean source of O(^{3}P). Initial reaction conditions ($[O]_0$ and $[C_3H_5]_0$) were determined from measured extents of depletion of SO_2 and allyl bromide, respectively,[12] and were chosen to yield [O] in large excess, $[O]_0/[C_3H_5]_0 > 20$. Under these conditions the O atom concentration was not significantly depleted by either the reaction under study or the relatively slow reaction between C_3H_5Br and O. C_3H_5 decays were monitored in time-resolved experiments.

The mechanism used to analyze the rate constant data consisted of reactions 2–4:

$$O + C_3H_5 \rightarrow \text{products} \qquad (2)$$

$$O \rightarrow \text{heterogeneous loss} \qquad (3)$$

$$C_3H_5 \rightarrow \text{heterogeneous loss} \qquad (4)$$

Because the oxygen atom concentration is not constant during an experiment (decreasing by as much as 20% during an experiment due to reaction 3), C_3H_5 decays were not purely exponential. The measured C_3H_5 decay profiles were fit to an analytical function derived from the above mechanism[11]

$$[C_3H_5]_t = [C_3H_5]_0 \exp(-k_4t) \exp[k'\{\exp(-k_3t) - 1\}/k_3], \quad k' = k_2[O]_0$$

Under each set of experimental conditions (T and P), the O atom decay constant (k_3) was measured (with C_3H_5Br absent) and the C_3H_5 heterogeneous loss rate constant k_4 was also determined (with SO_2 absent). The two values were incorporated into the fitting function before it was used to reproduce the measured C_3H_5 ion signal profile recorded when both reactants were present. Such a group of experiments yields the first-order C_3H_5 exponential decay constant for reaction 2 (k') that would have been measured had [O] remained at its initial value, $[O]_0$. The rate constant of reaction 2 was obtained from a set of experiments like the one describe above in which the initial O atom concentration was varied. A plot of k' vs $[O]_0$ for one such group of experiments is displayed in Figure 1 together with a typical measured C_3H_5 decay profile fitted to the function derived from the kinetic mechanism. k_2 was obtained from the slope of the line passing through the data.

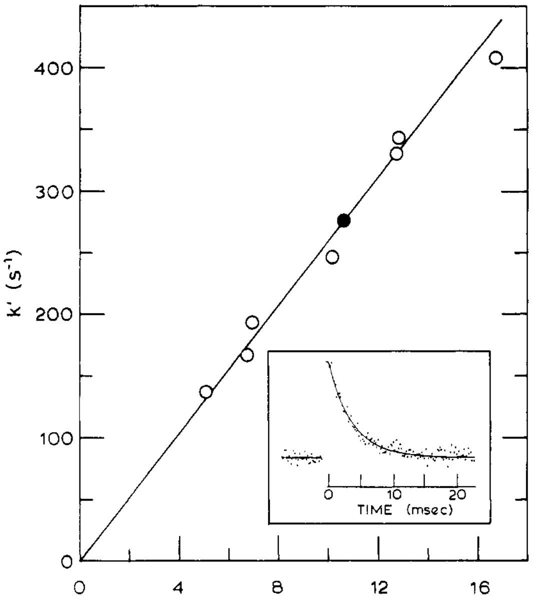

Figure 1. Plot of O + C_3H_5 first-order decay constants (k') vs $[O]_0$ for a set of experiments conducted at 600 K. [M] = 1.2×10^{17} molecules cm^{-3}. (See Table I for remaining conditions of these experiments.) Insert shows actual C_3H_5 decay profile recorded in these experiments at $[O]_0 = 1.07 \times 10^{12}$ molecules cm^{-3}. Line through data is the fitted function described in the text.

The mechanism and data analysis require the line to pass through the origin on the k'vs $[O]_0$ plot. The fact that the data indicate this behavior is partial confirmation that the mechanism used to interpret the experimental observations is complete. The conditions and results of all experiments are presented in Table I.

Before these experiments were begun, tests were conducted to verify that C_3H_5 did not react with SO_2 or SO. (Any significant reaction with SO would appear as an addition to the C_3H_5 + O rate constant.) Experiments were conducted at both 296 and 600 K to determine whether there is a measurable reaction between C_3H_5 and SO_2 under our experimental conditions. Photolysis of C_3H_5Br at 248 nm was used as the C_3H_5 source. (At this wavelength, SO_2 does not photodecompose to an observable degree but C_3H_5Br does.) No reaction of C_3H_5 with SO_2 was detected by using SO_2 concentrations comparable to those employed in rate constant experiments.

---

(12) Initial C_3H_5 concentrations were determined from measurements of the fraction of C_3H_5Br photolyzed by each laser pulse (typically 10%) and the assumption that C_3H_5 photolysis proceeds to an equal extent by the two routes shown in reaction 1. The estimated uncertainty in $[C_3H_5]_0$ is ±25%.

To test for the importance of the C_3H_5 + SO reaction, allyl bromide and SO_2 were photolyzed at 193 nm with C_3H_5 in large excess ($[C_3H_5] \gg [O]$ and [SO]). There was no observable depletion of SO as C_3H_5 reacted with O (and also by recombination and heterogeneous loss). The results of these tests indicate that the reaction rates of the C_3H_5 + SO and C_3H_5 + SO_2 reactions are negligible under the conditions used in the current investigation of the kinetics of reaction 2.

In addition to these tests, at each temperature, it was verified that the O + C_3H_5 rate constant was independent of $[C_3H_5Br]_0$, $[SO_2]_0$, and the laser fluence.

Finally, 1,5-hexadiene was used in one determination of the C_3H_5 + O rate constant to verify that the results obtained do not depend on the C_3H_5 source.

Photoionization in the mass spectrometer is provided by resonance lamps. Four energies were used in this investigation. A neon lamp (16.67, 16.85 eV) was used to detect O and SO_2, an argon lamp (11.62, 11.83 eV) to detect H_2CO and C_2H_4, a hydrogen lamp (10.2 eV) to photoionize SO, C_3H_5Br, H_2C_2O, C_3H_4, C_3H_5O, CH_3, C_2H_3, HCO, and C_2H_4O, and a chlorine lamp (8.9–9.1 eV) to photoionize C_3H_5.

The gases used were obtained from Linde (He, 99.995%), Matheson (SO_2, 99.98%), and Aldrich (C_3H_5Br, 99%; 1,5-hexadiene, 98%). Helium was used as provided. All other compounds were degassed by freeze–pump–thaw cycles prior to use.

3. Determination of C_3H_5 + O Reaction Mechanism. Products were searched for at both 298 and 600 K by use of two different photoionization energies (11.6 and 10.2 eV). These energies were adequate to ionize at least one of the products of all the reactive routes which are energetically possible. For a radical or molecule to be established as a primary reaction product, it not only had to be detected but also had to display the correct temporal behavior; i.e., it had to display an exponential growth constant which matched that of the decay of C_3H_5 (if it was a potential stable product) or grow and decay in the expected manner (if it was a potential radical product). Secondary products could be discriminated from primary ones by using this criterion. Secondary products displayed a delayed production onset and, when fit to the expected primary product exponential function, yielded "growth constants" that were substantially lower than that expected of a primary product.

The only species identified as a primary product was at mass 56, the mass number of an expected product, acrolein. This establishes the existence of the route

$$C_3H_5 + O \rightarrow C_3H_4O + H \qquad (2a)$$

(H atoms could not be detected by our photoionization mass spectrometer because of their high ionization potential.)

Other detectable products searched for but which were determined to be either absent or not primary products of the reaction include the molecular species H_2CO, H_2C_2O, C_2H_4, and C_3H_4, as well as the radicals CH_3, C_2H_3, HCO, and C_2H_4O. In one instance (C_3H_4), the potential product was also produced by the photolysis of the radical precursor, C_3H_5Br. In this case, the search was for a growth of its concentration above that which was produced instantly by the photolysis of the precursor.

The results of the product search indicate that reaction 2a is a major reactive route of the C_3H_5 + O reaction under the experimental conditions used in this investigation. A special effort was made to search for H_2CO, a product of a second anticipated reactive route (see Discussion), using very long ion counting times. None was detected. On the basis of the relative detection sensitivities for C_3H_5O and H_2CO, it can be concluded that the route that produces H_2CO, if present, is less than 20% as important as reaction 2a.

B. Studies Using Optical Spectroscopy To Monitor O and C_3H_5. Details of the apparatus and procedures used to measure atom + R reactions have been published[13] and are only summarized here. The unfocused 193-nm output ($\approx$3 Hz) of a Lumonics TE861S excimer laser was directed through the center of a heatable spherical stainless steel reactor. Gas in the photolysis region was replaced between laser pulses. The gas mixture comprised N_2O (O source, typically 0.01%), 1,5-hexadiene (C_3H_5 source, typically 0.002%), and the bath gas N_2 (>99.98%).

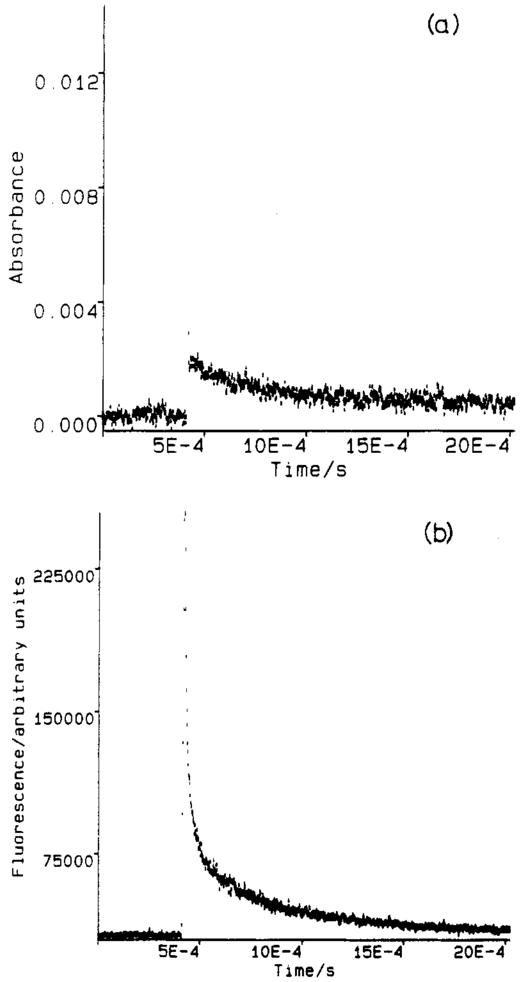

Figure 2. Typical decay profiles from optical spectroscopy measurements conducted at 500 K. (a) Time-resolved absorption signal for C_3H_5. (b) Time-resolved fluorescence signal for O. Total pressure = 100 Torr (N_2). $[C_6H_{10}] = 5.1 \times 10^{13}$ molecules cm^{-3}. $[N_2O] = 2.4 \times 10^{14}$ molecules cm^{-3}.

The gas was interrogated within the photolysis region, on a time scale at least 1000 times faster than that required for diffusion to the walls. O atom resonance radiation at 130 nm, from a microwave discharge in O_2/He, was directed into the cell. A solar blind photomultiplier tube viewed the fluorescence through a CaF_2 window in a direction at right angles to the exciting light.

Allyl was monitored in absorption at 223 nm, using a 150-W Xe/Hg lamp and a monochromator with a band-pass of 0.6 nm. The absorption band used is broad and structureless (fwhm = 10 nm[8]).

The two signals were amplified and then digitized simultaneously. Control experiments corrected for any distortion by scattered laser light (of the fluorescence trace) or laser radiofrequency noise (of the absorption trace). Usually, 1000 shots were summed before analysis. Figure 2 shows typical decay profiles.

1. 193-nm Photolysis of Precursors. The major photolysis products of N_2O ($\geq$95%) are $O(^1D) + N_2$.[14] $O(^1D)$ is deactivated to $O(^3P)$ by N_2 with a rate constant of $(2.8 \pm 0.3) \times 10^{-11}$ cm^3 molecule^{-1} s^{-1};[15] under experimental conditions, deactivation was complete in 20 ns.

---

[13] Brouard, M.; Macpherson, M. T.; Pilling, M. J. *J. Phys. Chem.* **1989**, *93*, 4047.

[14] Paraskevopoulos, G.; Cvetanovic, R. J. *J. Am. Chem. Soc.* **1969**, *91*, 7572.

[15] Schofield, K. *J. Photochem.* **1978**, *9*, 55.

The photolysis of 1,5-hexadiene was investigated by Tulloch et al.[8] The primary processes are production of two allyl radicals (68%), production of propene and propadiene (27%), with which O will react only slowly, and other minor routes (5%).

Using data for 193-nm photolysis of N_2O,[16] $[O]_0$ may be estimated at 3×10^{10} molecules cm^{-3} while $[C_3H_5]_0 = 1 \times 10^{13}$ molecules cm^{-3}. Under these conditions, loss of C_3H_5 by reaction with O and diffusion from the viewing zone is negligible, since $[C_3H_5]_0/[O]_0 \approx 300$, and C_3H_5 will diffuse even more slowly than O.

2. Measurement of Rate Constants. The C_3H_5 absorbance traces followed second-order kinetics, confirming the dominance of the recombination reaction

$$2C_3H_5 + M \rightarrow C_6H_{10} + M \qquad (5)$$

in the decay of C_3H_5. The time-dependent absorbance, Δ_t, is given by

$$(\Delta_t)^{-1} = (\Delta_0)^{-1} + 2(k_5/\sigma l)t$$

where Δ_0 is the zero time absorbance, σ is the absorption cross section at 223 nm, and l is the path length. Tulloch et al.[8] measured (k_5/σ) over the range 293–571 K, while van den Bergh and Callear determined σ.[17] The absorbance traces, which were obtained simultaneously with the oxygen atom fluorescence decays, were analyzed to determine Δ_0, using k_5/σ as a fixed parameter.

The oxygen atom decay is determined by three reactions:

$$O + C_3H_5 \rightarrow \text{products} \qquad (2)$$

$$O + C_6H_{10} \rightarrow \text{products} \qquad (6)$$

$$O \rightarrow \text{diffusion} \qquad (7)$$

Provided the allyl radical decays exclusively by recombination, then

$$[O]_t/[O]_0 = \exp\{-(k_6[C_6H_{10}] + k_7)t\}(1 + 2k_5[C_3H_5]_0t)^{-(k_2/\sigma)(\sigma/2k_5)}$$

Note that, given values for k_5/σ, analysis of the experimental decay profiles provides values of k_2/σ; i.e., the O + C_3H_5 rate constant is measured relative to the allyl radical absorption coefficient at 223 nm. Attempts were made to measure k_6 directly, but they were unsuccessful because of the dominance of reaction 2 even at low laser fluences. Ohta[18] has shown that the rate constant for the addition of OH to hexa-1,5-diene is twice that for addition to but-1-ene, to within ±7%, over a temperature range similar to that employed in the present experiments. k_6 was, therefore, equated to twice the rate constant for O + 1-C_4H_8,[19] giving

$$k_6 = 2.78 \times 10^{-11} \exp[-(335 \pm 101)\text{K}/T] \quad \text{cm}^3\ \text{molecule}^{-1}\ \text{s}^{-1}$$

k_7 was determined from separate experiments on N_2O/N_2 mixtures; the decays were sensibly exponential over the experimental time scale so that a first-order description of diffusive loss, with a time-independent value for k_7, is adequate. Typical pseudo-first-order loss rates for O were $k_2[C_3H_5]_0 \approx 1600$ s^{-1}, $k_6[C_6H_{10}] \approx 800$ s^{-1}, and $k_7 \approx 10$ s^{-1}. The measured values of k_2 were, therefore, sensitive to the chosen value of k_6; the uncertainties in k_2 which are quoted below reflect this sensitivity and have been calculated on the basis of a ±25% uncertainty in k_6. Experiments were conducted over a range of values of $[C_3H_5]_0$ ($(0.4-20) \times 10^{12}$ cm^{-3}), $[N_2]$ ($(1-12) \times 10^{18}$ cm^{-3}), laser energy (50–100 mJ total energy per pulse), and pulse frequency (1–3 Hz).

TABLE II: Conditions and Results of Experiments To Measure the C_3H_5 + O Rate Constant Using Optical Spectrometry

T, K	$10^{-18}[N_2]$, molecules cm^{-3}	$10^{-12}[C_3H_5]_0$, molecules cm^{-3}	no. of expts	$10^{10}k_2$,[a] cm^3 molecule^{-1} s^{-1}
296	1.7–11.7	0.4–12	67	2.3 ± 0.4
402	1.2–6.9	2.1–16	49	2.0 ± 0.5
500	0.96	2.3–16	67	3.0 ± 0.7
500	1.92	2.4–19	38	1.7 ± 0.5
500	3.84	0.4–21	60	2.5 ± 0.6

[a] These values for k_2 were obtained by using values of k_5 and σ from Tolluch et al.[8]

The results show no systematic dependence on $[C_3H_5]_0/[C_6H_{10}]$ which suggests that the rate constants assigned to reaction 6 are realistic.

The results obtained for k_2 are shown in Table II. The quoted uncertainties contain contributions from those in k_5/σ, σ, and k_6 and have been discussed with reference to the CH_3 + H reaction.[13] A full discussion of uncertainty contributions in the study of radical\radical reactions has also been reported by Macpherson et al.,[20] who considered in addition possible contributions from hot radical reactions. It was shown that, for CH_3, vibrational relaxation takes place on a microsecond time scale under the present experimental conditions. Hence, reaction before relaxation is very unlikely. Similar considerations apply for C_3H_5.

The materials used were obtained from BOC (N_2O, 99.6%; N_2, 99.999%) and Aldrich (C_6H_{10}, 98%). Nitrogen was used as provided. C_6H_{10} and N_2O were degassed by freeze–pump–thaw cycles before use. C_6H_{10} was stored over anhydrous $CaSO_4$.

III. Discussion

A. Rate Constant of the C_3H_5 + O Reaction. Given the difficulties of measuring atom + radical reaction rates and the differences in technique, there is satisfactory agreement between the two sets of results. The photoionization mass spectrometry results suggest a slight decrease in k_2 with temperature

$$k_2 = 2.3 \times 10^{-10} \exp(0.98\ \text{kJ mol}^{-1}/RT) \quad \text{cm}^3\ \text{molecule}^{-1}\ \text{s}^{-1}$$

although no such trend is discernible from absorption spectroscopy. Together the two sets of experiments demonstrate that k_2 is independent of pressure and a composite value of

$$k_2 = (3 \pm 1) \times 10^{-10} \quad \text{cm}^3\ \text{molecule}^{-1}\ \text{s}^{-1}$$

is recommended over the temperature range 300–600 K.

The magnitude of the C_3H_5 + O rate constant is that which would be expected for a "comparable" alkyl radical + O atom reaction. For free-radical reactions which proceed along an attractive potential, it has been demonstrated that, for an homologous series of reactions, log k (at a fixed temperature) is close to a linear function of the ionization potential (IP) of the radicals.[21-24] (Paltenghi et al. have provided a theoretical explanation for this correlation for reactions in which the addition process involves a curve crossing between the neutral and ionic surfaces.[21]) A plot of log k vs IP for the alkyl radical + O reactions is shown in Figure 3. k_2 is also plotted. It is apparent from the compliance of k_2 with this correlation that C_3H_5 reactivity in this C_3H_5 + R (R = $O(^3P)$) reaction is also not reduced by resonance stabilization.

B. Mechanism of the C_3H_5 + O Reaction. The magnitude of the rate constant, the absence of a pressure dependence over the range 2–350 Torr, and the observed production of acrolein suggest that the initial adduct, once formed, fragments irreversibly. The

---

[16] Okabe, H. *Photochemistry of Small Molecules*; Wiley-Interscience: New York, 1978.

[17] van den Bergh, H. E.; Callear, A. B. *Trans. Faraday Soc.* **1970**, *66*, 2681.

[18] Ohta, T. *J. Phys. Chem.* **1983**, *87*, 1209.

[19] Atkinson, R.; Pitts, J. N. *J. Chem. Phys.* **1977**, *67*, 38.

[20] Macpherson, M. T.; Pilling, M. J.; Smith, M. J. C. *J. Phys. Chem.* **1985**, *89*, 2268.

[21] Ruiz, R. P.; Bayes, K. D. *J. Phys. Chem.* **1984**, *88*, 2592.

[22] Paltenghi, R.; Ogryzlo, E. A.; Bayes, K. D. *J. Phys. Chem.* **1984**, *88*, 2595.

[23] Timonen, R. S.; Russell, J. J.; Sarzynski, D.; Gutman, D. *J. Phys. Chem.* **1987**, *91*, 1873.

[24] Loewenstein, L. M.; Anderson, J. G. *J. Phys. Chem.* **1985**, *89*, 5371.

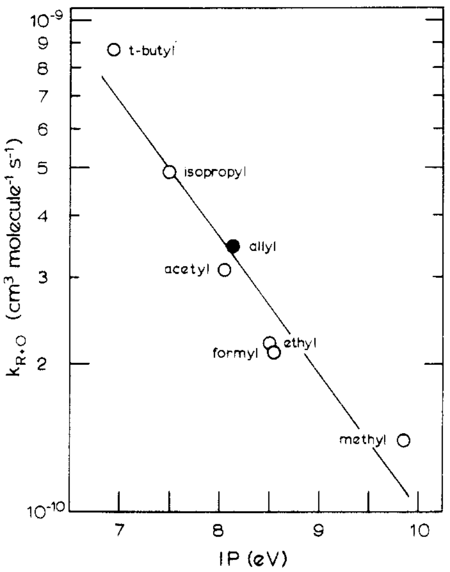

Figure 3. Plot of R + O rate constants vs ionization potential of R. Rate constants for R = alkyl and acyl radicals are taken from ref 28. The C_3H_5 + O rate constant is from the current study.

two most facile channels involve loss of H from the carbon atom which is bonded to O and fission of the adjacent C–C bond:

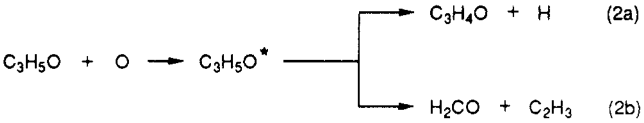

Neither C_2H_3 nor H_2CO was detected, suggesting that channel 2b is unimportant. Other possible channels involve rearrangement in $C_3H_5O^*$. For example, the following sets of products would be formed following H atom migration: $CH_3 + C_2H_2O$, $CH + C_2H_4O$, $C_2H_4 + HCO$, $C_3H_4 + OH$. That none of these products were observed, although not conclusive, is evidence that channel 2a is the major reaction route.

The products C_3H_4 + OH could also have been produced by a parallel direct H atom metathesis process. The fact that C_3H_4 was not produced at detectable levels indicates that this additional process, which is an important path in the alkyl radical + O atom reactions,[11,25-27] is an insignificant one in the case of the C_3H_5 + O reaction. This situation is not unexpected since abstraction would have involved removal of a vinylic hydrogen from a resonance-stabilized radical.

The absence of a pressure dependence for k_2 over the range of conditions covered by the two techniques, 2–350 Torr, indicates that the reaction proceeds irreversibly forward once the adduct is formed.

C. Conclusions. The reaction between C_3H_5 and $O(^3P)$ proceeds via an addition–elimination mechanism to form acrolein

$$C_3H_5 + O \rightarrow C_3H_4O + H \qquad (2a)$$

with $k_2 = (3 \pm 1) \times 10^{-10}$ cm^3 molecule^{-1} s^{-1} over the temperature range 300–600 K and at pressures between 2 and 350 Torr. There is no evidence for stabilization of the initial adduct, and other fragmentation channels contribute less than 10% to the reaction mechanism. Potential energy surface calculations of the adduct fragmentation and isomerization channels would provide an explanation for the dominance of this single route. With the use of other diagnostic probes (e.g., laser-induced fluorescence for OH), it should be possible to establish the importance of some of the minor channels of this reaction.

Acknowledgment. The research at C.U.A. was supported by the Division of Chemical Sciences, Office of Basic Energy Sciences, Office of Energy Research, U.S. Department of Energy, under Grant DE-FG02-87ER13733. SERC are thanked for their support through an equipment grant at Oxford and a research studentship to M.A.H.-L. This collaboration was made possible through NATO Research Grant 0518187, and this contribution is gratefully acknowledged.

Registry No. O, 17778-80-2; C_3H_5, 1981-80-2; C_3H_4O, 107-02-8; allyl bromide, 106-95-6; 1,5-hexadiene, 592-42-7.

---

(25) Hoyermann, K.; Sievert, R. *Symp. (Int.) Combust.* [*Proc.*], *17th* **1978**, 517.

(26) Lenhardt, T. M.; McDade, C. E.; Bayes, K. D. *J. Chem. Phys.* **1980**, *72*, 304.

(27) Washida, N. *Bull. Chem. Soc. Jpn.* **1987**, *60*, 3739.

(28) Miyoshi, A.; Matsui, H.; Washida, N. *J. Phys. Chem.* **1989**, *93*, 5813.

Effect of Viscosity and Rotor Size on the Dynamics of Twisted Intramolecular Charge Transfer

John D. Simon*,† **and Shyh-Gang Su**

Department of Chemistry B-041, University of California at San Diego, La Jolla, California 92093
(Received: September 18, 1989)

Picosecond emission spectroscopy is used to examine the kinetics of twisted intramolecular charge transfer in a series of symmetric bis((*N*,*N*-dialkylamino)phenyl) sulfones, DRAPS (R = methyl, propyl, and butyl), in alcohol solutions. Within a given solvent, the dynamics of charge transfer are not dependent on changes in the size of the rotating group; however, for a single molecule in the series of *n*-alcohols, the rate of charge transfer correlates with the inverse of the solvent viscosity. These seemingly contradictory observations are reconciled by taking into account polarity effects on the reaction barrier, thereby revealing that the rate of reaction for a single molecule in the series of alcohols is independent of changes in solvent viscosity.

Introduction

The importance of dynamic solvent effects on chemical reactions in polar solvent has been the subject of several recent experimental studies,[1-7] theoretical models,[8-17] and molecular dynamics simulations.[18] Central to most of these investigations is the understanding of the role of solvent friction on the chemical reaction

---

[†] NSF Presidential Young Investigator 1985–1990; Alfred P. Sloan Fellow 1988–1990; Camille and Henry Dreyfus Teacher-Scholar 1990–1995.

(1) (a) Simon, J. D.; Su, S. G. *J. Chem. Phys.* **1987**, *87*, 7016. (b) Simon, J. D.; Su, S. G. *J. Phys. Chem.* **1988**, *92*, 2395. (c) Su, S. G.; Simon, J. D. *J. Chem. Phys.* **1988**, *89*, 908. (d) Su, S. G.; Simon, J. D. *Chem. Phys. Lett.* **1989**, *158*, 423.

0022-3654/90/2094-3656$02.50/0